Magnetic Resonance Imaging Evaluation of Cardiac Masses

Maria Fernanda Braggion-Santos[1,3], Marcel Koenigkam-Santos[2,3], Sara Reis Teixeira[2], Gustavo Jardim Volpe[1,4], Henrique Simão Trad[2], André Schmidt[1]

Divisão de Cardiologia do Departamento de Clínica Médica - Hospital das Clínicas - Faculdade de Medicina de Ribeirão Preto, Universidade de São Paulo[1], Ribeirão Preto, SP; Centro de Ciências das Imagens e Física Médica - Hospital das Clínicas - Faculdade de Medicina de Ribeirão Preto da Universidade de São Paulo[2], Ribeirão Preto, SP - Brasil; Hospital Universitário - Universidade de Heidelberg[3], Heidelberg, Alemanha; Divisão de Cardiologia - Universidade Johns Hopkins[4], Baltimore, Estados Unidos

Abstract

Background: Cardiac tumors are extremely rare; however, when there is clinical suspicion, proper diagnostic evaluation is necessary to plan the most appropriate treatment. In this context, cardiovascular magnetic resonance imaging (CMRI) plays an important role, allowing a comprehensive characterization of such lesions.

Objective: To review cases referred to a CMRI Department for investigation of cardiac and paracardiac masses. To describe the positive case series with a brief review of the literature for each type of lesion and the role of cardiovascular magnetic resonance imaging in evaluation.

Methods: Between August 2008 and December 2011, all cases referred for CMRI with suspicion of tumor involving the heart were reviewed. Cases with positive histopathological diagnosis, clinical evolution or therapeutic response compatible with the clinical suspicion and imaging findings were selected.

Results: Among the 13 cases included in our study, eight (62%) had histopathological confirmation. We describe five benign tumors (myxomas, rhabdomyoma and fibromas), five malignancies (sarcoma, lymphoma, Richter syndrome involving the heart and metastatic disease) and three non-neoplastic lesions (pericardial cyst, intracardiac thrombus and infectious vegetation).

Conclusion: CMRI plays an important role in the evaluation of cardiac masses of non-neoplastic and neoplastic origin, contributing to a more accurate diagnosis in a noninvasive manner and assisting in treatment planning, allowing safe clinical follow-up with good reproducibility. (Arq Bras Cardiol. 2013;101(3):263-272)

Keywords: Heart Neoplasms / diagnosis; Magnetic Resonance Imaging; Myxoma; Sarcoma.

Introduction

Cardiac and paracardiac masses may be neoplastic or non-neoplastic. Primary cardiac neoplasms are rare, with an estimated prevalence of 0.001 to 0.03% in studies performed during necropsy[1]. Among the primary tumors 75% are benign, with myxomas being the most frequent lesions corresponding to more than half of the cases. The most prevalent primary malignant tumors are the cardiac sarcomas. Metastatic disease to the heart is 20 to 40 times more common than primary neoplasia, and 15% of patients with any type of cancer may present with cardiac metastases[2,3]. Among the differential diagnoses for neoplasia, intracardiac thrombus[4] is highlighted. However, a wide variety of lesions may represent a differentiated diagnosis for cardiac tumors, such as infectious processes, anatomic variations, focal myocardial hypertrophies and pericardiac cysts[5].

The imaging method most frequently used to assess a suspicious cardiac lesion is the transthoracic echocardiogram (TTE)[6,7] . However, in the last few years, cardiovascular magnetic resonance imaging (CMRI) has been established as an important tool in the identification and characterization of cardiac and paracardiac masses[8]. CMRI is a noninvasive exam, does not use ionizing radiation, has a wide field of view and has a high contrast resolution. The paramagnetic contrast agent (gadolinium) is safer and more effective when compared to iodinated contrast used in computed tomography (CT scan). CMRI also allows the evaluation of cardiac morphology and function in a single exam[9].

In this work, we reviewed the cases referred to our MRI service for investigation of cardiac and paracardiac masses. Cases with diagnostic confirmation were selected for presentation; the series is described along with a brief review of the literature for each type of tumor and the role of CMR in evaluation.

Mailing Address: Maria Fernanda Braggion Santos •
Neuenheimer Feld 370, 69120 Heidelberg, Germany
E-mail: ferbraggion@yahoo.com.br
Manuscript received October 01, 2012; revised manuscript October 15, 2012; accepted April 23, 2013.

DOI: 10.5935/abc.20130150

Methods

Between August 2008 and December 2011, 593 CMRI exams were performed in our service. All examinations and clinical data of the patients referred for investigation of cardiac masses were retrospectively reviewed. We selected cases of cardiac masses of neoplastic, benign or malignant nature, of primary or metastatic origin, as well as non-neoplastic lesions provided that they met the following criteria: 1) clinically appropriate exams and good quality images; 2) lesions confirmed by histopathology, or 3) lesions with therapeutic response and/or clinical evolution consistent with the clinical suspicion and imaging findings. All patients or legal guardians received the necessary information regarding the procedure to be performed, as well as the possible use of images in scientific papers, and signed an Informed Consent Form (ICF) prior to the exam.

The tests were performed using 1.5 Tesla MRI Equipment (Achieva, Philips Medical Systems, the Netherlands), using surface coils with phase arrangement and heart and respiratory synchronization (electrocardiogram - ECG vector). Gadolinium chelate (Gd) was used as the intravenous contrast agent and was administered by infusion pump in a dose appropriate for the patient's weight (0.1 to 0.2 mmol/kg). In all cases, a dedicated protocol was used for the assessment of cardiac masses, including morphological, functional and tissue characterization. This protocol was integrated into static sequences *T1 and* T2-weighted dark blood turbo spin-echo (TSE), with and without fat suppression, using dynamic sequences (cineMR) *gradient-echo* balanced with bright blood (*Balanced Steady State Free Precession*- bSSFP), sequences of post-contrast dynamic cardiac perfusion and images of late gadolinium enhancement (LGE). Images were obtained in conventional and complementary cardiac planes when necessary, and a physician experienced in cardiac imaging guided the performance of all exams (Table 1).

Results

Thirteen cases (2.2% of all tests performed in the period) were included in this study, which corresponded to a total of nine men with a mean age of 45 years. Table 2 summarizes the main clinical data for all patients. Eight (62%) patients had histopathological confirmation of the lesion, described as: one undifferentiated sarcoma, one rhabdomyoma, one cardiac fibroma, two atrial myxomas and three cases of secondary neoplastic involvement, one being a cardiac metastasis (parathyroid carcinoma), one involving direct intravascular extension (renal cell carcinoma of the right kidney) and one myocardial involvement caused by B cell lymphoma. Histopathological study was lacking for five (38%) patients: one fibroma, one pericardial cyst, one case of Richter's cardiac syndrome, one intra-atrial thrombus in a patient with cardiac amyloidosis and one case of infectious vegetation. These patients were included in the study because their lesions showed therapeutic response and/or clinical evolution consistent with clinical suspicion and imaging findings. Regarding etiology, six (46%) lesions were primary cardiac neoplasias, of which five (83%) were benign and only one was malignant. Among the five cases of malignant neoplasias involving the heart, four (80%) were not primary neoplasias. In three (23%) cases, examination by CMRI diagnosed non-neoplastic lesions.

Benign tumors

We found two cardiac myxomas in two different patients (Figure 1), one case showing an oval mass in the right atrium attached to the atrial septum (Figures 1A to 1D) and another showing a smaller and more irregular lesion, this one attached to the anterior leaflet of the mitral valve (Figures 1E to 1H). Both lesions showed heterogeneous signal and areas of high intensity best evidenced in LGE sequences; in the larger lesion, it was

Table 1 – Cardiovascular magnetic resonance imaging protocol for the assessment of cardiac masses

Sequence	Planes	Slice thickness / gap (mm)	RT/ET (ms)/FA (°)	Field of view (FOV) (cm)	Matrix of acquisition
Cine bSSFP Single slice	Long axis, short axis, 4-chamber, LV outflow tract	8.0/-	3.4/1.7/60	30-35	256x256
Cine bSSFP multiple slices	Short axis and 4-chamber	8.0/2.0	2.7/1.4/60	30-35	256x256
TSE T1 DIR dark blood with and without fat suppression	Short axis and/or four chambers	8.0/0.8	700-800/10/90	30-40	480x480
TSE T2 DIR dark blood	Short axis and/or four chambers	8.0/0.8	1,200-1,800/80/90	30-40	288x288
TSE 3IR	Short axis and/or four chambers	8.0/2.0	1,200-1,800/60/90	30-35	480x480
Resting perfusion post-Gd * (Ultrafast GRE)	Short axis (3-4 slices)	10.0/10.0	2.5/1.3/50	30-35	256x256
Late enhancement after 10-15 minutes (GRE Fast IR with suppression of normal myocardium)	Long axis, short axis and 4 chambers	10.0/0	6.1/3.0/25	30-35	512x512

RT: time of repetition; ET: echo time; FA: flip angle; FOV: field of view; bSSFP: balanced steady state free precession, LV: left ventricle; TSE: turbo spin echo; DIR: sequence with double inversion recovery for dark blood; 3IR: inversion recovery sequence with dark blood and fat suppression (triple inversion recovery); Gd: gadolinium chelate administered as an intravenous bolus dose of 0.1 mmol/kg; GRE: gradient echo.

Table 2 - Summary of clinical data of the patients studied by CMRI for the investigation of cardiac and paracardiac masses

Age (years)	Gender *	DIAGNOSIS	Clinical indication	Evolution
56	M	Atrial myxoma	Lesion identified on Echo after stroke evaluation	Surgical resection without complications
81	F	Atrial myxoma	Lesion identified during the evaluation of essential hypertension and atrial fibrillation by Echo	Surgical resection without complications
<1	F	Rhabdomyoma	Cardiac mass in antenatal ultrasonography	Death (cardiovascular complications during the late postoperative period)
10	M	Fibroma	Evaluation of cardiomegaly with suspicious finding on Echo	Lesion stable for more than 6 years
15	M	Fibroma	Evaluation of cardiomegaly with suspicious finding on Echo	Surgical resection without complications
42	M	Undifferentiated sarcoma	Cardiac mass identified on Echo during investigation of heart failure	Death (during chemotherapy)
34	M	Metastatic parathyroid carcinoma	Cardiac lesions identified on chest CT during restaging of the disease	Initial chemotherapy
54	M	Invasion of renal cell carcinoma	Renal mass invading the cardiac area	Initial local and systemic treatment
66	F	Richter's syndrome with cardiac involvement	Lesion identified on CT for restaging of the disease	Chemotherapy with partial response in recent control examinations
75	M	Intra-atrial thrombus in a patient with amyloidosis	Echo suggestive of amyloidosis in a patient with heart failure	Treatment with oral anticoagulation and appropriate response
44	F	Pericardial cyst	Finding of CT	Lesion stable in recent control examinations
67	M	Diffuse lymphoma of large B-cells	Cardiac mass identified on CT for restaging of the disease	Chemotherapy with partial response
35	M	Endocarditis	Vegetation attached to the papillary muscle visible on Echo after stroke in a patient with bone metastatic angiosarcoma	Antibiotic therapy with complete response

M: Male; Echo: echocardiography; F: Female; CT: Computed tomography.

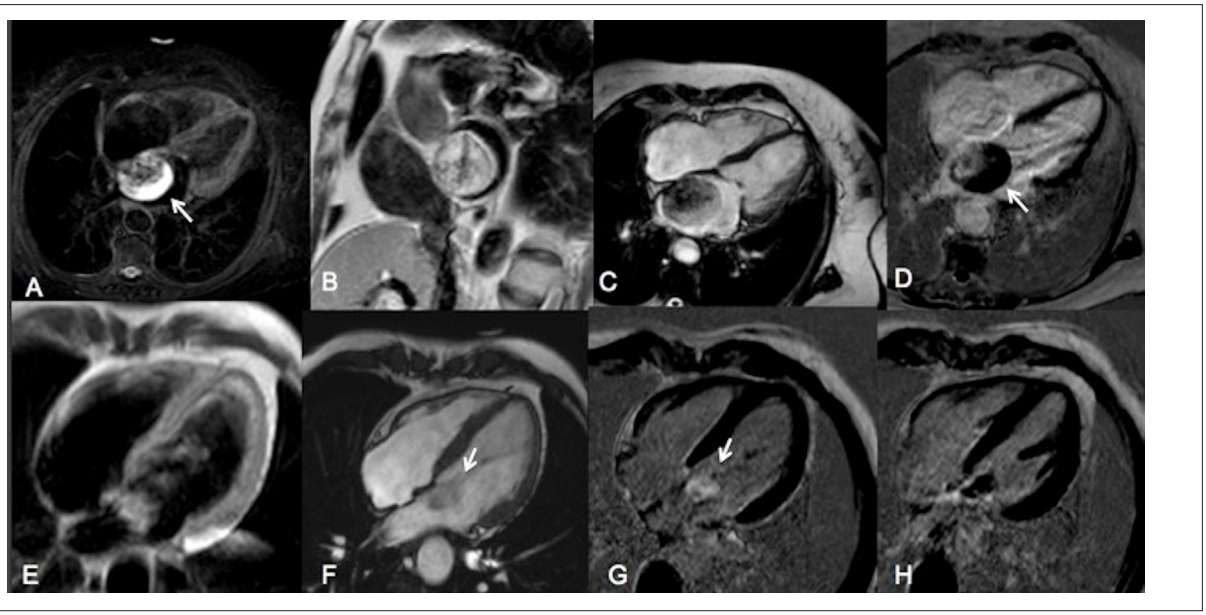

Figure 1 – *Cardiac myxomas in two different patients. First patient: image in four-chambers view, T2-weighted sequence with fat suppression (A), short-axis T1-weighted (B), four chambers bright blood SSFP (C) and LGE (D). The arrows show the hematic thrombus attached to the tumor. Second patient: images in four-chambers view, T1-weighted (E), SSFP (F) and LGE (G and H). The arrows show the component of the lesion that protrudes through the mitral valve.*

possible to notice a component of hematic thrombus attached to the surface of the lesion. Two patients were described having a cardiac fibroma (Figures 2A to 2F).In both cases, a well-defined oval mass on the wall of the left ventricle (LV) with a signal similar to the myocardium was identified, but with homogeneous intense signal on LGE sequences. In the case of cardiac rhabdomyoma (Figures 2G to 2I) we also found a well-defined mass on the LV wall, but with a prominent hyperintense signal on T2-weighted sequence and with no significant post-contrast enhancement.

Malignant tumors

In a patient with primary cardiac undifferentiated sarcoma (Figure 3), a partially bound infiltrative lesion is observed involving mainly the interventricular septum, with a slight hyperintense signal on T2-weighted sequence and heterogeneous post-contrast enhancement obliterating the ventricular cavities. CMRI showed functional impairment caused by the tumor, with reduced ventricular ejection fractions. Two patients are also described: one with cardiac involvement caused by diffuse lymphoma of large B cells (Figure 4) and one with Richter's syndrome (Figure 5). In both, infiltrative lesions with heterogeneous signal and enhancement in the myocardium are seen; the former involves mainly the anterolateral wall of the LV and the latter involves the atrial septum with extension to the pericardium. In the case of Richter's syndrome, it was also possible to identify the coronary arteries involved by the mass, with preserved shape and size, an aspect commonly described in mediastinal lymphomas. In addition, another two cases of secondary neoplastic involvement are described in the heart (Figure 6). In the patient

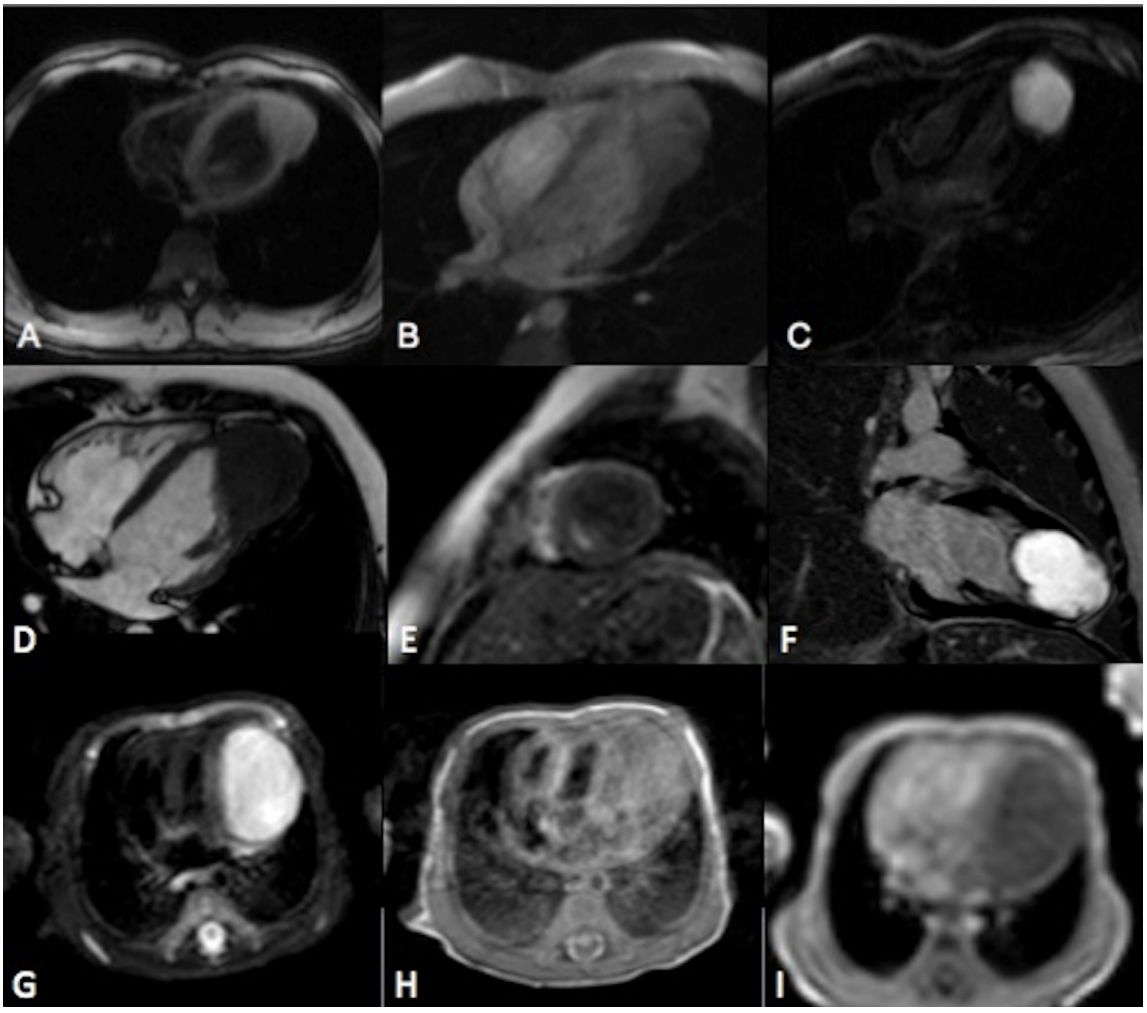

Figure 2 - *Fibromas and cardiac rhabdomyoma. Cardiac fibromas in two different patients. First patient: horizontal long axis T1-weighted image (A), post-contrast dynamic perfusion sequence (B) and LGE four-chambers view (C). Second patient: SSFP image in four-chambers view (D), perfusion sequence in short axis (E) and LGE in long axis (F). Cardiac rhabdomyoma: images in four-chambers view, T2-weighted sequence with fat suppression (G); perfusion sequence (H) and LGE (I).*

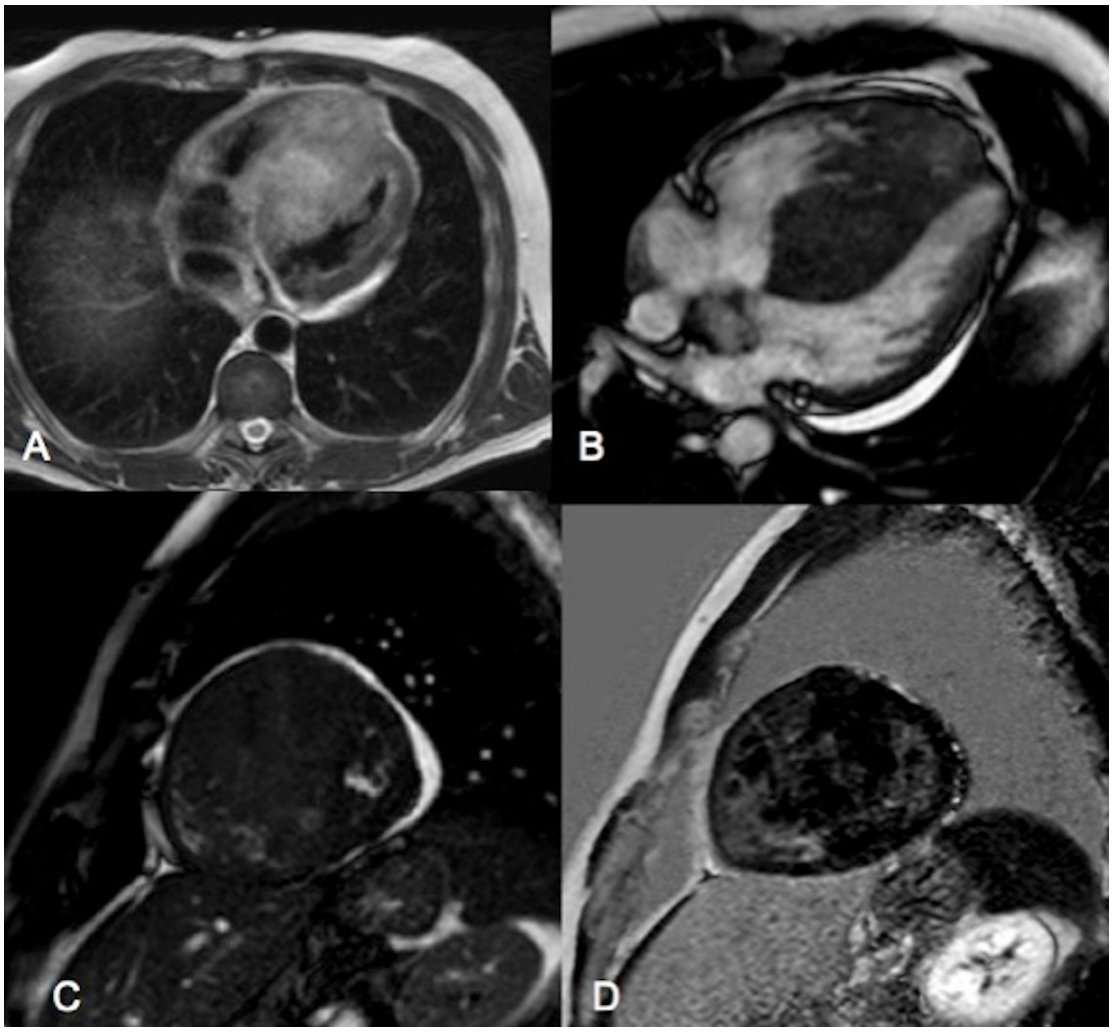

Figure 3 - *Undifferentiated cardiac sarcoma. Axial T2-weighted sequence (A), SSFP sequences in four-chambers (B) and short axis (C), sequence of LGE in the short axis (D).*

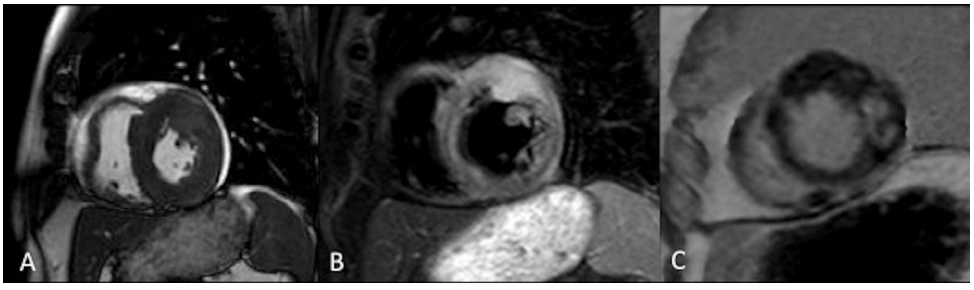

Figure 4 - *Secondary cardiac involvement by diffuse lymphoma of large B cells. Images in the short axis bright blood SSFP (A), T2-weighted sequence with fat suppression (B) and LGE sequence (C).*

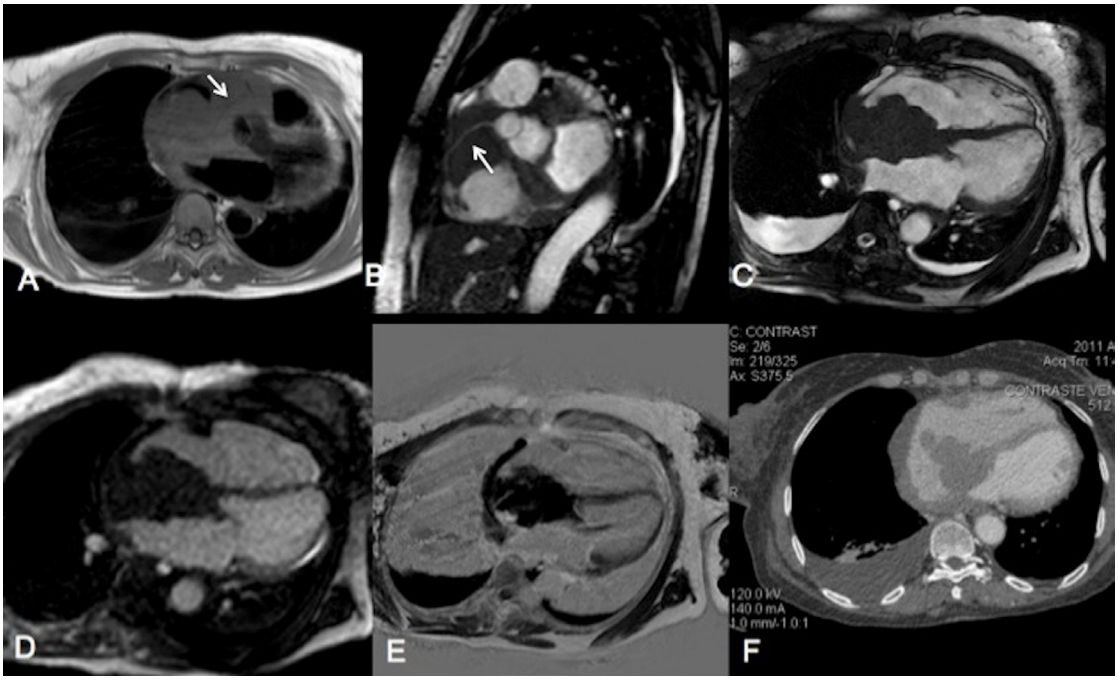

Figure 5 - *Richter's syndrome with cardiac involvement. Axial T1-weighted sequence (A), posterior short axis and four-chambers view SSFP (B and C), perfusion sequence four-chambers view (D) and LGE sequence (E). The arrows show the coronary arteries in the middle of the lesion. The follow-up exam post-treatment was performed with computed tomography (F) because of the other thoracic lesions and showed reduction of the lesion (partial response).*

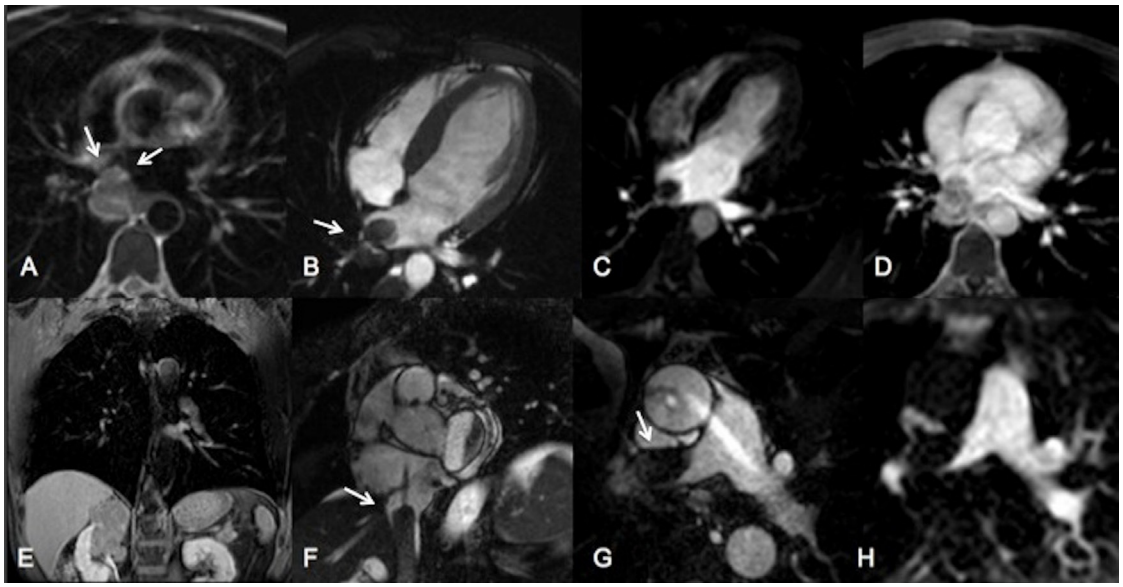

Figure 6 - *Secondary neoplastic involvement of the heart. Patient with metastatic parathyroid carcinoma; axial T2-weighted sequence (A), horizontal long axis SSFP and perfusion (B and C), axial tridimensional T1-weighted post-contrast sequence (D). The arrows show the involvement of the pulmonary veins. Patient with invasion of renal cell carcinoma of the right kidney; axial 3D T1-weighted post-contrast sequence (E), short axis SSFP (F), on the plane of bifurcation of the pulmonary artery SSFP (G) and perfusion sequence (H). The arrows show the thrombotic tumor component reaching the right atrium and the right pulmonary artery.*

with metastasis of parathyroid carcinoma, a heterogeneous irregular lesion is seen involving the posterior wall of the left atrium and the pulmonary veins. In the patient with invasion of renal cell carcinoma, a right renal mass is identified invading the lower vena cava, with tumor thrombus extending into the right atrium, passing through the tricuspid and pulmonary valves and reaching the right pulmonary artery, where it is associated with another thrombotic lesion.

Pseudotumoral lesions

In a patient with cardiac amyloidosis (Figures 7A to 7C), we identified a thrombus inside the left atrium attached to the wall, with low signal amid the bright blood and no areas of post-contrast enhancement. In this case, it was also possible to observe myocardial thickening with diffuse late enhancement, which is common in cardiac amyloidosis. One patient had infectious vegetation inside the LV (Figures 7D to 7F), characterized in CMRI as an intracavitary low-signal irregular lesion attached to the septal wall of the LV, with no areas of enhancement following injection of Gd. In the case of the pericardial cyst (Figures 7G to 7I), we observe the characteristic appearance of the lesion, which is lobulated with thin and incomplete septa, with homogeneous hyperintense signal on T2-weighted and without post-contrast enhancement, located adjacent to the right atrium and in contact with the pericardium sac.

Discussion

We describe here a series of 13 cases of cardiac and paracardiac masses studied by CMRI. The findings of this study are similar to those described in the medical literature regarding the incidence and characteristics of the lesions. Among the primary lesions, most were found to be benign lesions, with only one case of primary malignant neoplasia of the heart (a sarcoma, the most common type). In three cases, the CMRI identified non-neoplastic lesions, thereby helping to give the patients the appropriate treatment.

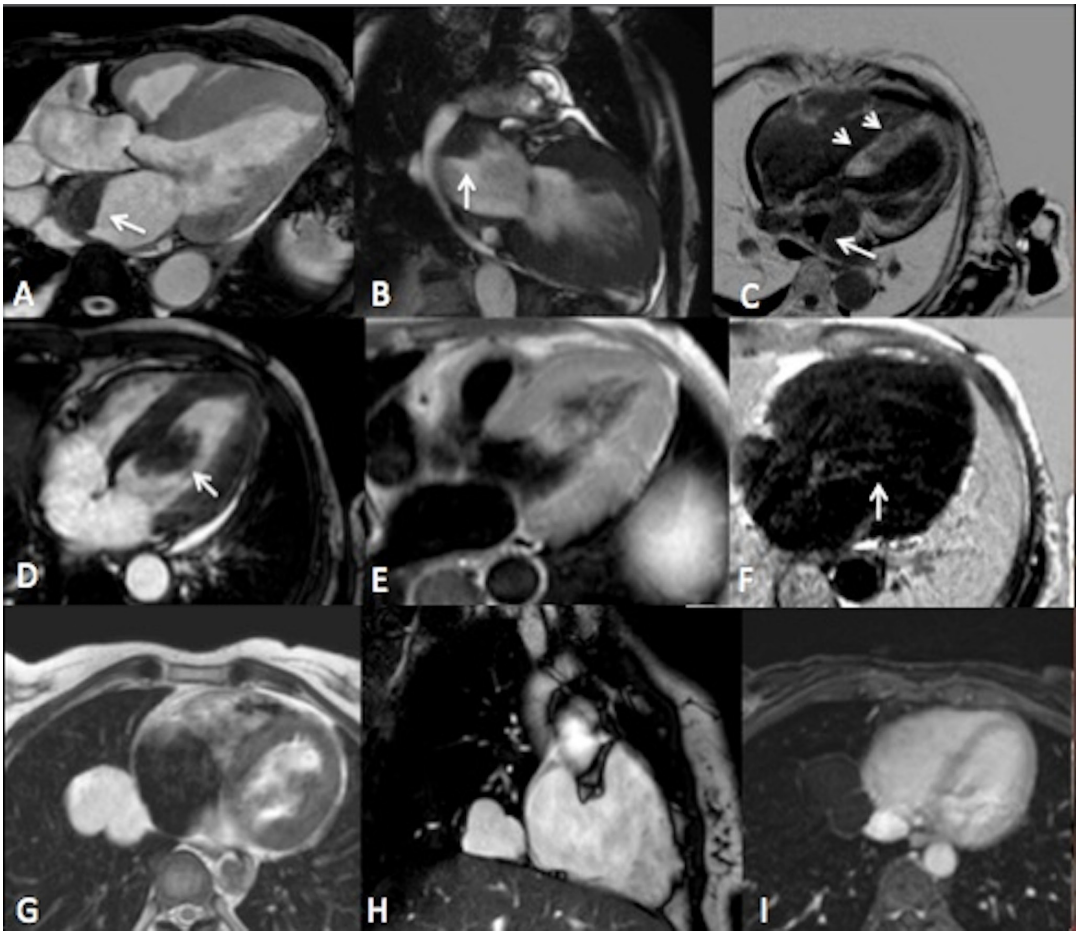

Figure 7 - *Non-neoplastic lesions. Patient with cardiac amyloidosis (arrowheads) and thrombus in the left atrium (arrows); SSFP images on the plane of the outflow tract of the left ventricle (A) and vertical long axis (B), sequence of LGE, four-chambers view (C). Patient with infectious vegetation inside the left ventricle (arrows); four-chambers view SSFP images (D), long-axis T1-weighted (E) and LGE four-chambers view (F). Pericardial cyst, axial T2-weighted image (G), SSFP long axis of the RV (H), axial three-dimensional T1-weighted post-contrast (I).*

Benign tumors

Two lesions were diagnosed as myxomas through CMRI examination, with histopathologic confirmation after surgical resection. Among the benign tumors, the cardiac myxoma represents the most common primary lesion affecting the heart. It is an endocardial mass which is generally mobile and connected to the interatrial septum by a narrow base, most commonly near the *fossa ovalis;* 75% of myxomas are located in the left atrium, 20% are found in the right atrium and a small percentage are found in the ventricles[10]. On CMRI, myxomas are well-defined, espheric or ovoid lobuled masses with heterogeneous signal intensity, usually isointense in relation to the adjacent myocardium on T1-weighted sequences, and hyperintense on T2-weighted sequences, depending on the content of the lesion. In addition to the myxoid material, the lesion may contain thrombus, necrotic or cystic material, calcified material or areas of acute or subacute hemorrhage[11]. After injection of Gd, heterogeneous enhancement helps to differentiate this lesion from cardiac thrombus, especially LGE sequences. Sequences of cineMR allow the demonstration of the precise location and mobility of the tumor, which may prolapse through the atrioventricular valves, most commonly the mitral valve[12].

Among the three patients under 20 years of age included in this study, one rhabdomyoma and two fibromas were diagnosed, which is in agreement with the two most common benign neoplasms in children and adolescents.

Rhabdomyoma is the most common primary cardiac tumor in children, accounting for over 60% of all primary cardiac neoplasms in this age group. The neoplasia originates in the myocardium and primarily affects the ventricles; it can be single or multiple and may be located in the intramyocardial or intracavitary areas, connected to the cardiac muscle[13]. On CMRI, the lesion has a solid and homogeneous appearance, isointense to the myocardium on T1-weighted sequences and hyperintense on T2-weighted sequences. LGE sequences do not show an important enhancement of this lesion.

Cardiac fibromas represent the second most common neoplasia in children and young adult patients. They are also found in the myocardium and typically present as a single well-defined lesion of intramyocardial location, most commonly in the interventricular septum[13]. On CMRI, the lesion is characterized as being isointense or discreetly hyperintense in relation to the myocardium on T1-weighted sequences, and hypointense on T2-weighted[14]. On LGE sequences, the fibromas present with intense and homogeneous enhancement, explained by the overflow and retention of the contrast material in the broad extracellular space which surrounds the fibrous tissue of the tumor[15]. Sometimes the lesion presents a central component of low signal intensity, which may be associated with calcifications[16]. The characteristics of T2-signal (hypointense) and LGE (prominently hyperintense) are the most specific in differentiating this lesion from cardiac rhabdomyoma[14,15].

Other benign neoplasias found in the heart are lipomas, papillary fibroelastomas and hemangiomas. Although not described in this study, knowledge of the main characteristics found on CMRI is important in differentiating among various cardiac lesions.

Lipomas are encapsulated lesions, usually located in the subendocardium, characterized on CMRI as hyperintense on T1-weighted and T2-weighted sequences, with an evident signal decrease in sequences with fat suppression. The papillary fibroelastomas are located preferentially on the mitral and aortic surfaces and may be pedunculated. On CMRI, they may present as lesions with high mobility on cineMR sequences, with intermediate signal intensity on T1-weighted sequences and hyperintense signal on T2-weighted sequences. The hemangiomas are usually located in the ventricles, present with an intermediary signal intensity on T1-weighted sequences, and are hyperintense on T2-weighted sequences. LGE images show hyperintense enhancement that may be heterogeneous due to the presence of calcifications and a fibrous septum inside the tumor[14].

The CMRI is not only highly accurate for the characterization of benign tumors, but is also able to provide important information regarding functional impairment and cardiac anatomical details in terms of surgical planning for the treatment of these lesions[9].

Malignant tumors

The only primary cardiac malignancy found in this study was an undifferentiated sarcoma. Sarcomas are neoplasias of mesenchymal origin that exhibit aggressive characteristics, usually with a fatal outcome. All types of sarcoma can be found in the heart, angiosarcoma is the most common in adults (37%), usually located in the right atrium. There are also undifferentiated sarcomas (24%), leiomyosarcomas (8%), fibrosarcomas (5%) and osteosarcomas (3-9%), these are most commonly found in the left atrium[17]. On CMRI exam, they are generally large and heterogeneous with ill-defined margins, frequently occupying almost the entire affected chamber or multiple chambers of the heart. Pericardial or extracardiac structures invasion or valvular destruction may be identified. The pericardial involvement can be seen through the presence of effusion, thickening or nodules in the membrane. The signal intensity in these types of tumors is heterogeneous, generally intermediate on T1-weighted sequences and hyperintense on T2-weighted sequences; enhancement after administration of Gd is also heterogeneous[11]. Cardiac lymphoma is another primary malignancy of the heart, but these are extremely rare and affect mainly immunosuppressed individuals. They are mostly non-Hodgkin B-cell type and preferentially involve the right atrium, with invasion of adjacent structures and voluminous pericardial effusion[11].

In the remaining four cases of malignancies involving the heart, there were different neoplasms resulting in secondary cardiac involvement. These findings are consistent with the data described in the literature[2].

Richter's syndrome is a rare complication of chronic lymphocytic leukemia (CLL) of B cells, occurring in 2 to 8%

of cases, which consists in the formation of a rapidly growing mass, constituting a high grade non-Hodgkin lymphoma. This syndrome has a very poor prognosis and the clinical signs and symptoms are not specific, making diagnosis difficult, especially in the early stages of transformation. New tests have been studied to more easily detect Richter's syndrome in patients with CLL, including imaging studies[18].

The cardiac metastases have pericardial effusion as the most common manifestation of cardiac involvement. Lung neoplasms most commonly metastasize to the heart. Other primary tumors that can metastasize to the heart are: breast, kidney and esophageal carcinomas, melanomas, lymphomas and leukemias[2,3]. Heart involvement may occur in several ways, such as through direct invasion, lymphatic involvement, hematogenic dissemination or tumor transvenous extension. Lung neoplasms usually invade the heart directly. Lymphomas, leukemias and melanomas usually involve the heart by hematogenous dissemination, while renal cell carcinoma involves more frequently in the right atrium, through the dissemination of a tumor thrombus via the inferior vena cava. Metastases do not have a specific appearance on CMRI, but most of them show hypointense signal on T1-weighted sequences and hyperintense signal on T2-weighted sequences. The exception is melanoma, which may present hyperintense signal on T1-weighted sequence because of the paramagnetic properties of melanin. Almost all types of metastatic lesions present post-contrast enhancement[14].

Despite the lower specificity of CMRI in the differentiation of types of malignancy involving the heart, the exam can provide important information for the local staging of the lesion (precise location, dimensions in different axes, the presence of invasion of adjacent structures and cardiac functional impairment), in addition to the follow-up over the course of treatment in a non-invasive way and without using ionizing radiation or iodinated contrast media[15].

Pseudotumoral lesions

Finally, three non-neoplastic lesions were diagnosed by CMRI exam: one intracardiac thrombus, one pericardial cyst and one infective vegetative lesion.

Thrombi are the lesions that are most frequently confused with cardiac neoplasms. Typically, these are located in the left atrium and are related to the presence of atrial fibrillation; when diagnosed in the LV, they occur in patients as sequelae of myocardial infarction, Chagas cardiomyopathy with LV apical aneurysm or severe ventricular dysfunction of any etiology. In CMRI, the signal intensity of thrombi vary according to their "age" and the phase of hemoglobin degradation. Acute thrombi present hyperintense signal on T1 and T2-weighted sequences, while subacute thrombi are hyperintense on T1-weighted sequences but have low signal intensity on T2 weighted sequences. Organized chronic thrombi present low-signal intensity on T1 and T2-weighted sequences due to the presence of hemosiderin deposits[19,20]. Perfusion images and LGE are most important in differentiating tumors from thrombi, since neoplastic lesions present with a vascularized tissue component that enhances after contrast, while there is no enhancement in hematic thrombi. Very rarely, old organized thrombi can enhance due to the presence of fibrotic tissue, but the other morphological and signal characteristics identified on CMRI help to differentiate them from tumors[9].

Pericardial cysts are congenital malformations, which are rare, usually localized in the right costophrenic angle (70% of cases). They are usually diagnosed as an incidental finding on chest radiographs or echocardiograms. The CMRI examination shows a paracardiac, homogeneous, well-defined structure with low or intermediate signal intensity on T1-weighted sequences and hyperintense signal on T2-weighted sequences. The T1 signal of the cyst depends on its content; when "dense" or highly proteic it may present with a high signal on T1-weighted sequence. The pericardial cyst does not enhance after administration of Gd and CMRI is the best exam to characterize the cystic nature of the lesion, in addition to providing detailed information as to its location, size and relation with the heart and other adjacent structures[21].

The most frequently used tests to confirm the diagnosis of infective endocarditis are the TTE and TEE (transesophageal echocardiogram). CMRI may be useful in patients with limited-quality images on echocardiogram, and also in patients in whom it is not possible to perform a transesophageal exam. CMRI complement the evaluation of infectious vegetations by permitting the identification of perivalvular extension of the lesions, as well as locating abscesses and characterizing lesions in locations where a suitable evaluation was not possible by ecocardiogram[22].

Conclusion

Cardiac tumors are rare; however, the differentiation of non-neoplastic lesions from neoplastic ones and a correct identification of the type of lesion is essential for appropriate therapeutic planning. In this aspect, CMRI is of great importance since it is a noninvasive exam and offers a wide field of view and superior tissue characterization, without the using iodinated contrast media or ionizing radiation. Besides the important diagnostic role and its usefulness in the choice of treatment, often eliminating the need for biopsy, CMRI may be indicated for patients follow-up with cardiac neoplasms, representing a safe and high reproducible method.

Author contributions

Conception and design of the research: Braggion-Santos MF, Koenigkam-Santos M, Volpe GJ, Trad HS, Schmidt A; Acquisition of data: Braggion-Santos MF, Koenigkam-Santos M, Teixeira SR, Volpe GJ, Trad HS; Analysis and interpretation of the data: Braggion-Santos MF, Koenigkam-Santos M, Teixeira SR, Volpe GJ, Trad HS, Schmidt A; Writing of the manuscript: Braggion-Santos MF, Koenigkam-Santos M, Teixeira SR; Critical revision of the manuscript for intellectual content: Koenigkam-Santos M, Schmidt A.

Potential Conflict of Interest

No potential conflict of interest relevant to this article was reported.

Study Association

This study is not associated with any post-graduation program.

Sources of Funding

There were no external funding sources for this study.

References

1. Reynen K. Frequency of primary tumors of the heart. Am J Cardiol. 1996;77(1):107.
2. Bussani R, De-Giorgio F, Abbate A, Silvestri F. Cardiac metastases. J Clin Pathol. 2007;60(1):27-34
3. MacGee W. Metastatic and invasive tumors involving the heart in a geriatric population: a necropsy study. Virchows Arch A Pathol Anat Histopathol. 1991;419(3):183-9.
4. Srichai MB, Junor C, Rodriguez LL, Stillman AE, Grimm RA, Lieber ML, et al. Clinical, imaging, and pathological characteristics of left ventricular thrombus: a comparison of contrast- enhanced magnetic resonance imaging, transthoracic echocardiography, and transesophageal echocardiography with surgical or pathological validation. Am Heart J. 2006;152(1):75-84.
5. Dawson D, Mohiaddin R. Assessment of pericardial diseases and cardiac masses with cardiovascular magnetic resonance. Prog Cardiovasc Dis. 2011;54(3):305-19.
6. Butany J, Nair V, Naseemuddin A, Nair GM, Catton C, Yau T. Cardiac tumours: diagnosis and management. Lancet Oncol. 2005;6(4):219-28.
7. Peters PJ, Reinhardt S. The echocardiographic evaluation of intracardiac masses: a review. J Am Soc Echocardiogr. 2006;19(2):230-40.
8. Altbach MI, Squire SW, Kudithipudi V, Castellano L, Sorrell VL. Cardiac MRI is complementary to echocardiography in the assessment of cardiac masses. Echocardiography. 2007;24(3):286-300.
9. Sparrow PJ, Kurian JB, Jones TR, Sivananthan MU. MR imaging of cardiac tumors. Radiographics. 2005;25(5):1255-76.
10. Burke AP, Virmani R. Cardiac myxoma: a clinicopathologic study. Am J Clin Pathol. 1993;100(6):671-80.
11. Grebenc ML, Rosado-de-Christenson ML, Green CE, Burke AP, Galvin JR. Cardiac myxoma: imaging features in 83 patients. Radiographics. 2002;22(3):673-89.
12. Grebenc ML, Rosado de Christenson ML, Burke AP, Green CE, Galvin JR. Primary cardiac and pericardial neoplasms: radiologic-pathologic correlation. Radiographics. 2000;20(4):1073-103.
13. Uzun O, Wilson DG, Vujanic GM, Parsons JM, De Giovanni JV. Cardiac tumours in children. Orphanet J Rare Dis. 2007;1:2-11.
14. O'Donnell DH, Abbara S, Chaithiraphan V, Yared K, Killeen RP, Cury RC, et al. Cardiac tumors: optimal cardiac MR sequences and spectrum of imaging appearances. Am J Roentgenol. 2009;193(2):377-87.
15. Beroukhim RS, Prakash A, Buechel ER, Cava JR, Dorfman AL, Festa P, et al. Characterization of cardiac tumors in children by cardiovascular magnetic resonance imaging: a multicenter experience. J Am Coll Cardiol. 2011;58(10):1044-54.
16. De Cobelli F, Esposito A, Mellone R, Papa M, Varisco T, Besana R, et al. Images in cardiovascular medicine. Late enhancement of a left ventricular cardiac fibroma assessed with gadolinium-enhanced cardiovascular magnetic resonance. Circulation. 2005;112(13):e242-3.
17. Burke AP, Cowan D, Virmani R. Primary sarcomas of the heart. Cancer. 1992;69(2):387-95.
18. Bruzzi JF, Macapinlac H, Tsimberidou AM, Truong MT, Keating MJ, Marom EM, et al. Detection of Richter's transformation of chronic lymphocytic leukemia by PET/CT. J Nucl Med. 2006;47(8):1267-73.
19. Paydarfar D, Krieger D, Dib N, Blair RH, Pastore JO, Stetz JJ Jr, et al. In vivo magnetic resonance imaging and surgical histopathology of intracardiac masses: distinct features of subacute thrombi. Cardiology. 2001;95(1):40-7.
20. Barkhausen J, Hunold P, Eggebrecht H, Schüler WO, Sabin GV, Erbel R, et al. Detection and characterization of intracardiac thrombi on MR imaging. AJR Am J Roentgenol. 2002;179(6):1539-44.
21. Yared K, Baggish AL, Picard MH, Hoffmann U, Hung J. Multimodality imaging of pericardial diseases. JACC Cardiovasc Imaging. 2010;3(6):650-60.
22. Vilacosta I, Gómez J. Complementary role of MRI in infectious endocarditis. Echocardiography. 1995;12(6):673-6.